Journal of Alloys and Compounds 488 (2009) 13–17

Contents lists available at ScienceDirect

Journal of Alloys and Compounds

journal homepage: www.elsevier.com/locate/jallcom

Synthesis and magnetic properties of $(Pr_{1-x}Sm_x)_5Fe_{17}$ ($x = 0–1$) phase

Tetsuji Saito*, Tomokazu Furutani

Department of Mechanical Science and Engineering, Chiba Institute of Technology, 2-17-1 Tsudanuma, Narashino, Chiba 275-0016, Japan

ARTICLE INFO

Article history:
Received 28 April 2009
Received in revised form 18 August 2009
Accepted 18 August 2009
Available online 25 August 2009

Keywords:
Permanent magnets
Intermetallics
Liquid quenching
Magnetic measurements

ABSTRACT

An investigation of the synthesis of the $(Pr_{1-x}Sm_x)_5Fe_{17}$ ($x = 0–1$) phase and its magnetic properties is presented. $(Pr_{1-x}Sm_x)_5Fe_{17}$ melt-spun ribbons were obtained that partly or mostly consisted of the amorphous phase and showed low coercivity. It was found that the $(Pr,Sm)_5Fe_{17}$ phase could be produced by annealing of the $(Pr_{1-x}Sm_x)_5Fe_{17}$ melt-spun ribbons, regardless of the Sm content of the phase. The remanence and coercivity of the annealed melt-spun ribbons were highly dependent on both the annealing temperature and the Sm content of the $(Pr_{1-x}Sm_x)_5Fe_{17}$ alloy. The highest remanence of 46.4 emu/g was achieved in the $(Pr_{0.2}Sm_{0.8})_5Fe_{17}$ melt-spun ribbon annealed at 1073 K for 1 h, while the highest coercivity was achieved in the Sm_5Fe_{17} melt-spun ribbon annealed at 973 K for 1 h.

1. Introduction

The search for magnetic materials has extended to the frontiers of physics and material science. With the appearance of high-energy-product Nd–Fe–B permanent magnets, the research and development of permanent magnetic materials has mainly concentrated on alloys containing rare-earths [1,2]. Intensive research on these alloys has shown that the Nd_5Fe_{17} phase is a stable intermetallic compound in the binary Nd–Fe system [3–5]. The crystal structure of Nd_5Fe_{17} belongs to the hexagonal space group $P6_3/mcm$. Although the Nd_5Fe_{17} phase has a high saturation magnetization of 1.61 T at 4 K and a Curie temperature above 500 K, it does not possess c-axis anisotropy, which is essential for permanent magnet materials [6]. The R_5Fe_{17} (R: rare-earth) structure can be obtained with various rare-earth elements, as found with other rare-earth compounds such as the $R_2Fe_{14}B$ phase [7]. In fact, the magnetic phase found in Sm–Fe–Ti alloys was characterized by Stadelmaier et al. [8] as isostructural with the Nd_5Fe_{17} phase. Since Sm has a Stevens factor αj with a different sign from that of Nd, the Sm_5Fe_{17} phase is expected to show c-axis anisotropy. Only the formation of the Sm_5Fe_{17} phase has been reported in sputtered Sm–Fe films, and the films exhibited a large coercivity of 14.7 kOe [9,10]. Since the formation of several metastable phases has been reported in binary Sm–Fe alloys, the Sm_5Fe_{17} phase may be produced by rapid solidification processing such as melt-spinning [11]. Recent studies have revealed, however, that the Sm_5Fe_{17} phase can be obtained by annealing of Sm–Fe melt-spun ribbon [12,13]. In this study, $(Pr_{1-x}Sm_x)_{15}Fe_{17}$ ($x = 0–1$) alloys were produced by the melt-spinning technique. The purpose of this study was to seek the possibility of producing the $(Pr_{1-x}Sm_x)_{15}Fe_{17}$ ($x = 0–1$) phase by annealing of the melt-spun ribbons. A systematic investigation of the structures and the magnetic properties of these compounds was performed.

2. Experimental

$(Pr_{1-x}Sm_x)_5Fe_{17}$ ($x = 0–1$) alloy ingots were prepared by induction melting under an argon atmosphere. An alloy ingot of 20 g was induction melted under an argon atmosphere in a quartz crucible having an orifice 0.6 mm in diameter at the bottom. The molten metal was ejected through the orifice with argon onto a chromium-plated copper wheel rotating at a surface velocity of 50 ms^{-1}. The resultant melt-spun ribbons were wrapped with tantalum foils and annealed under an argon atmosphere at temperatures between 773 K and 1173 K for 1 h. The phases in the specimens were examined by X-ray diffraction (XRD) using Cu Kα radiation. The thermomagnetic curves of the specimens were examined using a vibrating sample magnetometer (VSM) with an applied field of 500 Oe. The magnetic properties of the specimens were measured at room temperature by both the VSM with a maximum applied field of 25 kOe and a superconducting quantum interference device (SQUID) magnetometer with a maximum applied field of 70 kOe. No demagnetization correction was made in the hysteresis curve.

3. Results and discussion

Fig. 1 shows the XRD patterns of the $(Pr_{1-x}Sm_x)_5Fe_{17}$ ($x = 0–1$) melt-spun ribbons. Narrow and broad diffraction peaks can be seen in the XRD patterns of the Pr_5Fe_{17} alloy. The Pr_5Fe_{17} alloy consisted of the Pr_2Fe_{17} and $PrFe_2$ phases. Unlike the XRD pattern of the Pr_5Fe_{17} alloy, small diffraction peaks are noted in the XRD patterns of the $(Pr_{0.8}Sm_{0.2})_5Fe_{17}$ and $(Pr_{0.6}Sm_{0.4})_5Fe_{17}$ alloys. Although these peaks are somewhat weak and broad, these diffraction peaks are considered to be the $(Pr,Sm)_2Fe_{17}$ and $(Pr,Sm)Fe_2$ phases. Unlike

* Corresponding author. Tel.: +81 47 478 0315; fax: +81 47 478 0329.
E-mail address: tetsuji.saito@it-chiba.ac.jp (T. Saito).

0925-8388/$ – see front matter © 2009 Elsevier B.V. All rights reserved.
doi:10.1016/j.jallcom.2009.08.074

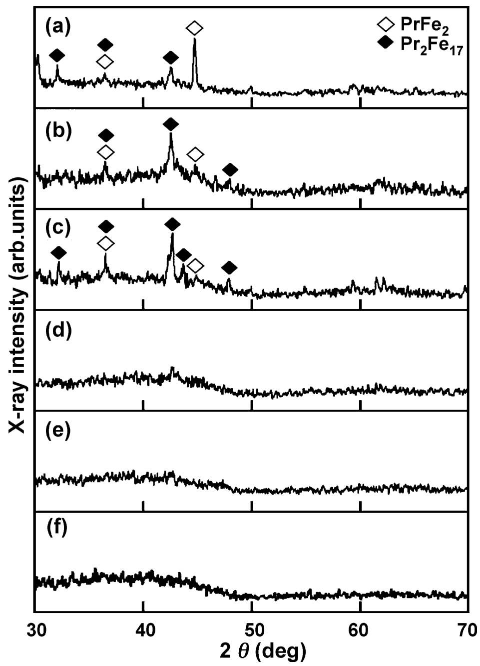

Fig. 1. XRD patterns of Pr–Sm–Fe melt-spun ribbons: (a) Pr_5Fe_{17}, (b) $(Pr_{0.8}Sm_{0.2})_5Fe_{17}$, (c) $(Pr_{0.6}Sm_{0.4})_5Fe_{17}$, (d) $(Pr_{0.4}Sm_{0.6})_5Fe_{17}$, (e) $(Pr_{0.2}Sm_{0.8})_5Fe_{17}$, and (f) Sm_5Fe_{17} alloy.

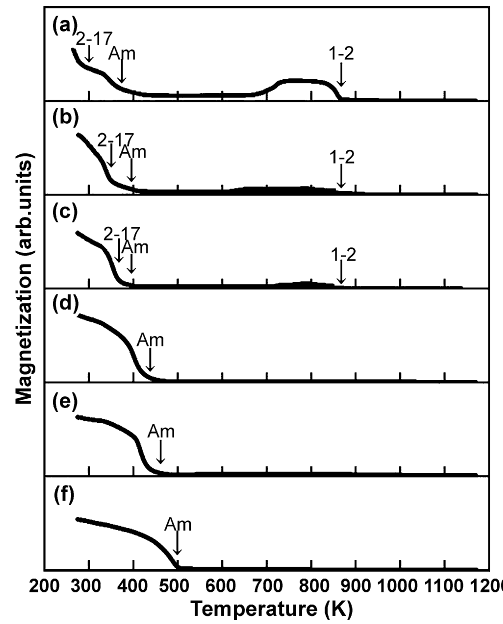

Fig. 2. Thermomagnetic curves of Pr–Sm–Fe melt-spun ribbons: (a) Pr_5Fe_{17}, (b) $(Pr_{0.8}Sm_{0.2})_5Fe_{17}$, (c) $(Pr_{0.6}Sm_{0.4})_5Fe_{17}$, (d) $(Pr_{0.4}Sm_{0.6})_5Fe_{17}$, (e) $(Pr_{0.2}Sm_{0.8})_5Fe_{17}$, and (f) Sm_5Fe_{17} alloy.

the XRD pattern of the $(Pr_{0.6}Sm_{0.4})_5Fe_{17}$ alloy, small diffraction peaks are noted in the XRD pattern of the $(Pr_{0.4}Sm_{0.6})_5Fe_{17}$ alloy. These peaks are embedded in a halo-like peak and are too weak to be indexed to any crystalline phase. The XRD pattern of the $(Pr_{0.2}Sm_{0.8})_5Fe_{17}$ alloy shows a fairly broad halo-like peak, which is characteristic of an amorphous structure. Virtually the same XRD pattern is obtained for the Sm_5Fe_{17} alloy. This indicates that the increased Sm content in the $(Pr_{1-x}Sm_x)_{15}Fe_{17}$ alloy markedly increases the glass formability.

In order to identify the magnetic phase in the $(Pr_{1-x}Sm_x)_5Fe_{17}$ (x = 0–1) melt-spun ribbons, their thermomagnetic curves were examined. The results of the thermomagnetic studies are shown in Fig. 2. The thermomagnetic curve of the Pr_5Fe_{17} alloy shows two large magnetic transitions at around 300 K and 860 K and a small magnetic transition at around 370 K. This suggests that the Pr_5Fe_{17} alloy consist of three different magnetic phases. According to the results of the XRD studies, this specimen consisted of the Pr_2Fe_{17} and $PrFe_2$ phases. Thus, the two large magnetic transitions should correspond to the Curie temperatures of these phases. No report on the Curie temperature of the $PrFe_2$ phase is found, whereas the Curie temperature of the Pr_2Fe_{17} phase is reported to be 293 K [14]. The magnetic transition at around 300 K corresponds to the Curie temperature of the Pr_2Fe_{17} phase and the magnetic transition at around 860 K is believed to correspond to the Curie temperature of the $PrFe_2$ phase. The small magnetic transition at around 370 K is supposed to be the Curie temperature of the amorphous phase. The thermomagnetic curves of the $(Pr_{1-x}Sm_x)_5Fe_{17}$ (x = 0.2–0.4) alloys are similar to that of the Pr_5Fe_{17} alloy. This indicates that the $(Pr_{1-x}Sm_x)_5Fe_{17}$ (x = 0.2–0.4) alloys also consist of the $(Pr,Sm)_2Fe_{17}$ and $(Pr,Sm)Fe_2$ phases, together with the amorphous phase. On the other hand, the thermomagnetic curves of the $(Pr_{1-x}Sm_x)_5Fe_{17}$ (x = 0.6–1.0) alloys show one magnetic transition temperature. According to the results of the XRD studies, these specimens consisted of the amorphous phase. Thus, the observed magnetic transition corresponds to the Curie temperature of amorphous Pr–Sm–Fe alloy. The magnetic transition temperature becomes higher with increasing Sm content in the $(Pr_{1-x}Sm_x)_5Fe_{17}$ (x = 0.6–1.0) alloys.

The $(Pr_{1-x}Sm_x)_5Fe_{17}$ (x = 0–1) melt-spun ribbons were either amorphous or partially amorphous and exhibited low coercivity values regardless of the Sm content. It is known that crystalline phases can be produced by rapid solidification processing and subsequent heat treatment. Thus, the $(Pr_{1-x}Sm_x)_5Fe_{17}$ (x = 0–1) melt-spun ribbons were annealed at temperatures between 773 K and 1173 K for 1 h. Fig. 3 shows the dependence of the coercivity of the $(Pr_{1-x}Sm_x)_5Fe_{17}$ (x = 0–1) melt-spun ribbons on the annealing temperature. The specimens annealed at 773 K exhibit a coercivity value as low as that of the amorphous melt-spun ribbon. The coercivity of the Pr_5Fe_{17} and $(Pr_{0.8}Sm_{0.2})_5Fe_{17}$ alloys is not changed by annealing. This indicates that the small substitution of Sm for Pr in the annealed Pr_5Fe_{17} alloy does not result in an increase in coer-

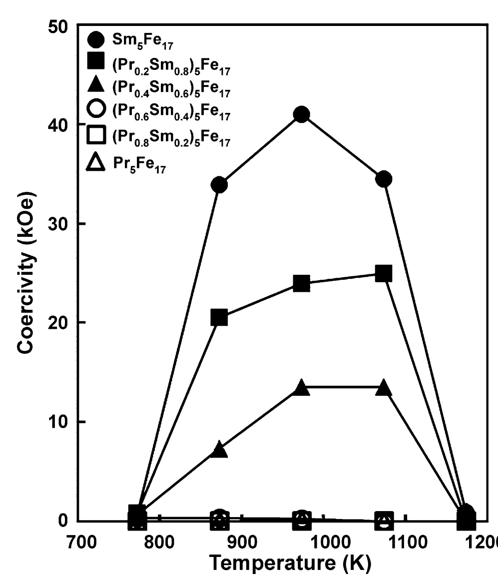

Fig. 3. Dependence of the coercivity of $(Pr_{1-x}Sm_x)_{15}Fe_{17}$ (x = 0–1) melt-spun ribbons on the annealing temperature.

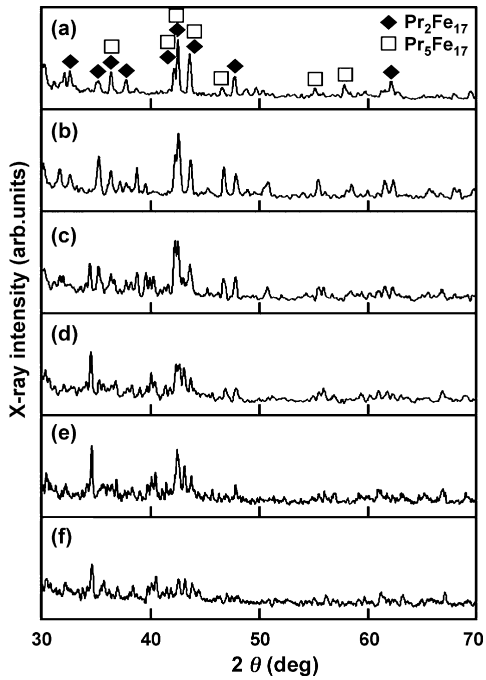

Fig. 4. XRD patterns of Pr–Sm–Fe melt-spun ribbons annealed at 873 K for 1 h: (a) Pr_5Fe_{17}, (b) $(Pr_{0.8}Sm_{0.2})_5Fe_{17}$, (c) $(Pr_{0.6}Sm_{0.4})_5Fe_{17}$, (d) $(Pr_{0.4}Sm_{0.6})_5Fe_{17}$, (e) $(Pr_{0.2}Sm_{0.8})_5Fe_{17}$, and (f) Sm_5Fe_{17} alloy.

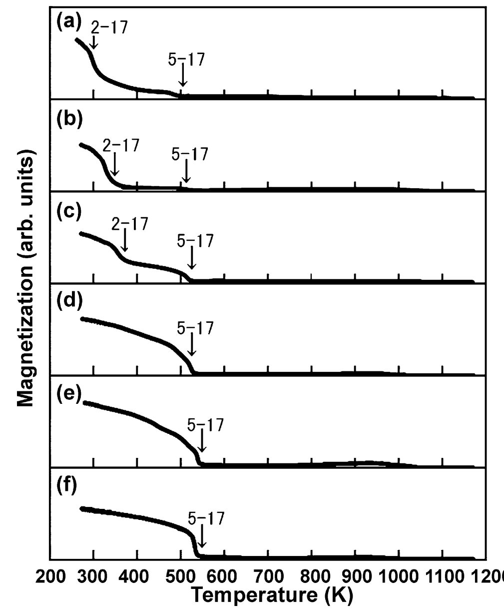

Fig. 5. Thermomagnetic curves of Pr–Sm–Fe melt-spun ribbons annealed at 873 K for 1 h: (a) Pr_5Fe_{17}, (b) $(Pr_{0.8}Sm_{0.2})_5Fe_{17}$, (c) $(Pr_{0.6}Sm_{0.4})_5Fe_{17}$, (d) $(Pr_{0.4}Sm_{0.6})_5Fe_{17}$, (e) $(Pr_{0.2}Sm_{0.8})_5Fe_{17}$, and (f) Sm_5Fe_{17} alloy.

civity. However, the coercivity of the $(Pr_{1-x}Sm_x)_5Fe_{17}$ alloys with $x = 0.6$ or higher increases sharply as the annealing temperature increases. This indicates that the relatively large substitution of Sm for Pr in the annealed Pr_5Fe_{17} alloy results in an increase in coercivity. This is due to the formation of the hard magnetic phase formed during the annealing of the $(Pr_{1-x}Sm_x)_5Fe_{17}$ ($x = 0$–1) melt-spun ribbons.

The structures of the annealed $(Pr_{1-x}Sm_x)_5Fe_{17}$ ($x = 0$–1) melt-spun ribbons were then examined by XRD and thermomagnetic studies. Fig. 4 shows the XRD patterns of the $(Pr_{1-x}Sm_x)_5Fe_{17}$ ($x = 0$–1) melt-spun ribbons annealed at 873 K for 1 h. The corresponding thermomagnetic curves are shown in Fig. 5. According to the equilibrium phase diagram, a Sm_5Fe_{17} alloy at equilibrium exists in the two phase region of Sm_2Fe_{17} and $SmFe_3$ phases. A Pr_5Fe_{17} alloy at equilibrium exists in the two phase region of Pr_2Fe_{17} and Pr phases. The Pr_5Fe_{17} alloy showed diffraction peaks that may be assigned to the Pr_5Fe_{17} phase together with the Pr_2Fe_{17} phase. Since the XRD pattern of the Pr_5Fe_{17} phase is similar in appearance to that of the Pr_2Fe_{17} phase, it is difficult to distinguish these phases in the Pr_5Fe_{17} alloy. Unlike in the XRD studies, clear changes in the magnetic transition temperature are noted in the thermomagnetic curve of the Pr_5Fe_{17} alloy, with two magnetic transitions seen at around 300 K and 500 K. This indicates that the Pr_5Fe_{17} alloy consists of two different magnetic phases. These magnetic transitions are believed to correspond to the Curie temperatures of the Pr_5Fe_{17} and Pr_2Fe_{17} phases. Since it is known that the magnetic transition at around 300 K corresponds to the Curie temperature of the Pr_2Fe_{17} phase, the other magnetic transition is considered to be the Curie temperature of the Pr_5Fe_{17} phase. Although the Pr_5Fe_{17} phase is not the equilibrium phase but the metastable phase, the Pr_5Fe_{17} phase is formed during the annealing of the Pr_5Fe_{17} melt-spun ribbon. The thermomagnetic curves of the annealed $(Pr_{1-x}Sm_x)_5Fe_{17}$ ($x = 0.2$–0.4) alloys are similar to that of the Pr_5Fe_{17} alloy. These magnetic transition temperatures become higher with increasing Sm content in the annealed $(Pr_{1-x}Sm_x)_5Fe_{17}$ ($x = 0.2$–0.4) alloys. This indicates that the substitution of Sm for Pr in the annealed $(Pr_{1-x}Sm_x)_5Fe_{17}$ ($x = 0.2$–0.4) alloys leads to an increase in the magnetic transition temperature of both the Pr_2Fe_{17} and Pr_5Fe_{17} phases. On the other hand, the thermomagnetic curve shows one magnetic transition temperature when the $(Pr_{1-x}Sm_x)_5Fe_{17}$ alloys contain a relatively large amount of Sm. The observed magnetic transition is considered to be the Curie temperature of the $(Pr_{1-x}Sm_x)_5Fe_{17}$ ($x = 0.6$–1) phase. This indicates that a large substitution of Sm for Pr promotes the formation of the metastable $(Pr,Sm)_5Fe_{17}$ phase.

Changes in the magnetic phase can be more effectively determined by thermomagnetic studies than XRD studies. Further studies were therefore carried out by thermomagnetic measurements. The results are shown in Figs. 6–8. It was found that the magnetic phases in the annealed $(Pr_{1-x}Sm_x)_5Fe_{17}$ ($x = 0$–1) alloys

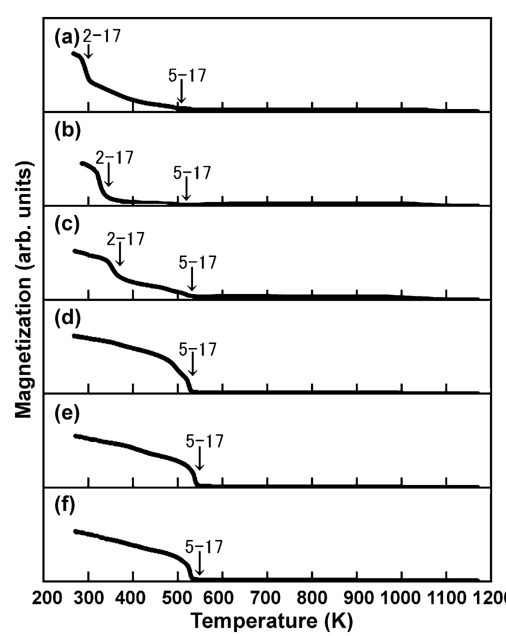

Fig. 6. Thermomagnetic curves of Pr–Sm–Fe melt-spun ribbons annealed at 973 K for 1 h: (a) Pr_5Fe_{17}, (b) $(Pr_{0.8}Sm_{0.2})_5Fe_{17}$, (c) $(Pr_{0.6}Sm_{0.4})_5Fe_{17}$, (d) $(Pr_{0.4}Sm_{0.6})_5Fe_{17}$, (e) $(Pr_{0.2}Sm_{0.8})_5Fe_{17}$, and (f) Sm_5Fe_{17} alloy.

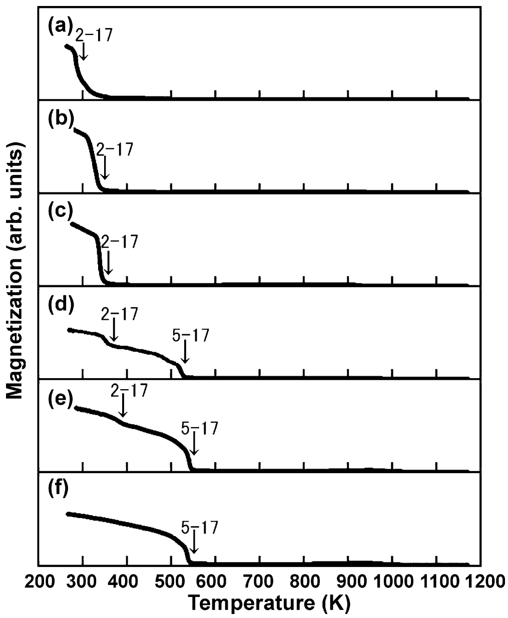

Fig. 7. Thermomagnetic curves of Pr–Sm–Fe melt-spun ribbons annealed at 1073 K for 1 h: (a) Pr_5Fe_{17}, (b) $(Pr_{0.8}Sm_{0.2})_5Fe_{17}$, (c) $(Pr_{0.6}Sm_{0.4})_5Fe_{17}$, (d) $(Pr_{0.4}Sm_{0.6})_5Fe_{17}$, (e) $(Pr_{0.2}Sm_{0.8})_5Fe_{17}$, and (f) Sm_5Fe_{17} alloy.

were dependent on both the Sm content of the alloy and the annealing temperature. The $(Pr_{1-x}Sm_x)_5Fe_{17}$ alloys with $x = 0.4$ or lower consist of the $(Pr,Sm)_2Fe_{17}$ and $(Pr,Sm)_5Fe_{17}$ phases when annealed at 873 K and 973 K, but only the $(Pr,Sm)_2Fe_{17}$ phase when annealed at 1073 K and 1173 K. Although the $(Pr_{1-x}Sm_x)_5Fe_{17}$ alloys with $x = 0.4$ or lower contain some $(Pr,Sm)_5Fe_{17}$ phase, when annealed at 873 K and 973 K, the main phase in the annealed $(Pr_{1-x}Sm_x)_5Fe_{17}$ alloys is the soft magnetic $(Pr,Sm)_2Fe_{17}$ phase. On the other hand, the $(Pr_{1-x}Sm_x)_5Fe_{17}$ alloys with $x = 0.6$ or higher consist only of the $(Pr,Sm)_5Fe_{17}$ phase when annealed at 873 K and 973 K. These results indicate that the increased coercivity in the annealed alloys with $x = 0.6$ or higher is due to the formation of the metastable $(Pr,Sm)_5Fe_{17}$ phase. The $(Pr_{1-x}Sm_x)_5Fe_{17}$ alloys with $x = 0.6$ and 0.8 consist of the $(Pr,Sm)_5Fe_{17}$ phase together with the $(Pr,Sm)_2Fe_{17}$ phase when annealed at 1073 K, but the Sm_5Fe_{17} alloy consists only of the Sm_5Fe_{17} phase when annealed at 1073 K. This is why the Sm_5Fe_{17} alloy exhibited a larger coercivity than the $(Pr_{1-x}Sm_x)_5Fe_{17}$ alloys with $x = 0.6$ and 0.8. However, the $(Pr_{1-x}Sm_x)_5Fe_{17}$ alloys with $x = 0.6$ consist of the $(Pr,Sm)_2Fe_{17}$ phase, while those with $x = 0.8$ or higher consist of the $(Pr,Sm)_2Fe_{17}$ and $(Pr,Sm)Fe_3$ phases when annealed at 1173 K. At higher annealing temperatures, the formation of the equilibrium phase such as $(Pr,Sm)_2Fe_{17}$ and $(Pr,Sm)Fe_3$ phases is favored compared to that of the metastable $(Pr,Sm)_5Fe_{17}$ phase. Although the $(PrSm)_5Fe_{17}$ phase is metastable, this phase is stable for longer annealing time (up to 3 h) at 1073 K. However, annealing at 1173 K for 1 h resulted in the decomposition of the $(PrSm)_5Fe_{17}$ phase.

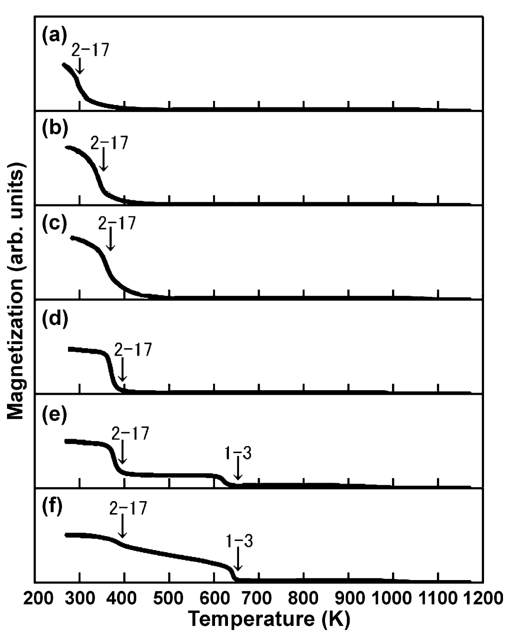

Fig. 8. Thermomagnetic curves of Pr–Sm–Fe melt-spun ribbons annealed at 1173 K for 1 h: (a) Pr_5Fe_{17}, (b) $(Pr_{0.8}Sm_{0.2})_5Fe_{17}$, (c) $(Pr_{0.6}Sm_{0.4})_5Fe_{17}$, (d) $(Pr_{0.4}Sm_{0.6})_5Fe_{17}$, (e) $(Pr_{0.2}Sm_{0.8})_5Fe_{17}$, and (f) Sm_5Fe_{17} alloy.

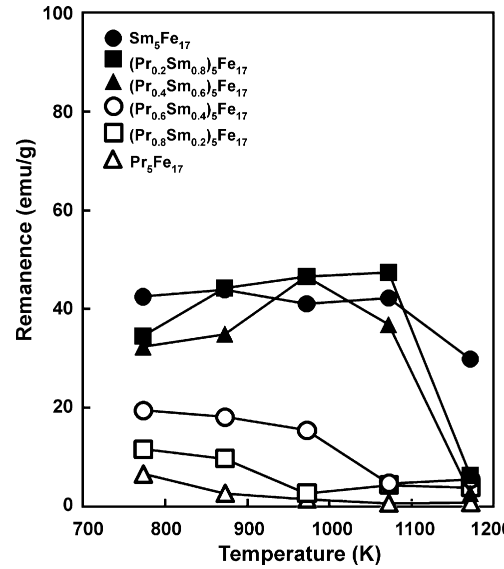

Fig. 9. Dependence of the remanence of $(Pr_{1-x}Sm_x)_{15}Fe_{17}$ ($x = 0$–1) melt-spun ribbons on the annealing temperature.

Fig. 9 shows the dependence of the remanence of the $(Pr_{1-x}Sm_x)_5Fe_{17}$ ($x = 0$–1) melt-spun ribbons on the annealing temperature. The remanence of the $(Pr_{1-x}Sm_x)_5Fe_{17}$ ($x = 0$–0.4) alloys increases with increasing Sm content. On the other hand, the remanence of the $(Pr_{1-x}Sm_x)_5Fe_{17}$ ($x = 0.6$–1) alloys increases up to 1073 K and then decreases as the Sm content increases. Unlike the case of the coercivity of the annealed $(Pr_{1-x}Sm_x)_5Fe_{17}$ alloys with $x = 0.6$ or higher, the increase in remanence is relatively small. The maximum remanence is achieved in the $(Pr_{0.2}Sm_{0.8})_5Fe_{17}$ alloy annealed at 1073 K. The demagnetization curve of the $(Pr_{0.2}Sm_{0.8})_5Fe_{17}$ melt-spun ribbon annealed at 1073 K is shown in Fig. 10. For comparison, the demagnetization curve of the Sm_5Fe_{17} melt-spun ribbon annealed at 973 K is also shown. The Sm_5Fe_{17}

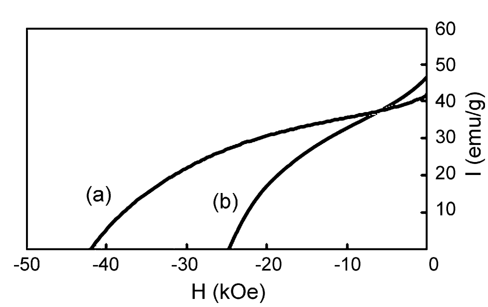

Fig. 10. Demagnetization curves of (a) Sm_5Fe_{17} melt-spun ribbon annealed at 973 K for 1 h and (b) $(Pr_{0.2}Sm_{0.8})_{15}Fe_{17}$ melt-spun ribbon annealed at 1073 K for 1 h.

melt-spun ribbon annealed at 973 K exhibited a large coercivity of 41.9 kOe with a remanence of 41.7 emu/g. The annealed $(Pr_{0.2}Sm_{0.8})_5Fe_{17}$ melt-spun ribbon exhibited an attractively high coercivity of 25 kOe, with a higher remanence of 46.4 emu/g than the annealed Sm_5Fe_{17} melt-spun ribbon. Although the remanence of the annealed $(Pr_{0.2}Sm_{0.8})_5Fe_{17}$ melt-spun ribbon is not yet comparable to that of Nd–Fe–B melt-spun ribbon, the annealed Sm–Fe melt-spun ribbon exhibits a much higher coercivity than Nd–Fe–B melt-spun ribbon [2].

4. Conclusion

$(Pr_{1-x}Sm_x)_5Fe_{17}$ (x = 0–1) melt-spun ribbons were obtained that partly or mostly consisted of the amorphous phase and showed low coercivity. Heat treatment of the melt-spun ribbons at 873–1073 K for 1 h resulted in formation of the metastable $(Pr,Sm)_5Fe_{17}$ phase. The amount of the metastable $(Pr,Sm)_5Fe_{17}$ phase was limited in the annealed $(Pr_{1-x}Sm_x)_5Fe_{17}$ (x = 0–0.4) melt-spun ribbons and showed low coercivity. On the other hand, the annealed $(Pr_{1-x}Sm_x)_5Fe_{17}$ (x = 0.6–1) melt-spun ribbons consisted mainly of the metastable $(Pr,Sm)_5Fe_{17}$ phase together with a small amount of the $(Pr,Sm)Fe_3$ phase and exhibited large coercivity. A coercivity of 41.9 kOe was achieved in the Sm_5Fe_{17} melt-spun ribbon annealed at 973 K for 1 h. However, the $(Pr_{1-x}Sm_x)_5Fe_{17}$ (x = 0–1) melt-spun ribbons annealed at 1273 K did not contain the $(Pr,Sm)_5Fe_{17}$ phase and showed low coercivity regardless of the Sm content. The $(Pr_{0.2}Sm_{0.8})_5Fe_{17}$ melt-spun ribbon annealed at 1073 K exhibited the highest remanence of 46.4 emu/g with a coercivity of 25 kOe.

Acknowledgement

This work was supported by a Grant-in-Aid for Special Purposes (No. 20900139) from the Japan Society for the Promotion of Science. The use of the facilities of the Materials Design and Characterization Laboratory at the Institute for Solid State Physics, the University of Tokyo, is gratefully acknowledged.

References

[1] M. Sagawa, S. Fujimura, N. Togawa, H. Yamamoto, Y. Matsuura, J. Appl. Phys. 55 (1984) 2083.
[2] J.J. Croat, J.F. Herbst, R.W. Lee, F.E. Pinkerton, J. Appl. Phys. 55 (1984) 2078.
[3] G.C. Hadjipanayis, A. Tsoukatos, J. Strzeszewski, G.J. Long, O.A. Pringle, J. Magn. Magn. Mater. 78 (1989) L1.
[4] G. Schneider, F.J.G. Landgraf, F.P. Missell, J. Less-Common Met. 153 (1989) 169.
[5] T. Saito, S. Ozawa, T. Motegi, J. Appl. Phys. 91 (2002) 8828.
[6] F.J.G. Landgraf, F.P. Missell, H.R. Rechenberg, V. Villas-Boas, J.M. Moreau, L. Paccard, J.P. Nozieres, J. Appl. Phys. 70 (1991) 6125.
[7] F.J. Cadieu, H. Hegde, R. Rani, A. Navarathna, K. Chen, Mater. Lett. 11 (1991) 284.
[8] H.H. Stadelmaier, G. Schneider, E.T. Henig, M. Ellner, Mater. Lett. 10 (1991) 303.
[9] A. C. Neiva and F. P. Missell, in: C.A.F. Manwaring (Ed.), Proceedings of the 8th International Symposium on Magnetic Anisotropy and Coercivity, 1994, pp. 315–324.
[10] T. Saito, J. Alloys Compd. 440 (2007) 315.
[11] T. Saito, Scripta Mater. 57 (2007) 457.
[12] F.J.G. Landgraf, G. Schneider, V. Villas-Boas, F.P. Missell, J. Less-Common Met. 163 (1990) 209.
[13] J.M. Moreau, L. Paccard, J.P. Nozieres, F.P. Missell, G. Schneider, V. Villas-Boas, J. Less-Common Met. 163 (1990) 245.
[14] F.A.O. Carbral, S. Gama, J. Less-Common Met. 167 (1990) 31.